Stem Cell Reports
Report
ISSCR
OPEN ACCESS

H1foo Has a Pivotal Role in Qualifying Induced Pluripotent Stem Cells

Akira Kunitomi,[1] Shinsuke Yuasa,[1,*] Fumihiro Sugiyama,[2] Yuki Saito,[1] Tomohisa Seki,[1] Dai Kusumoto,[1] Shin Kashimura,[1] Makoto Takei,[1] Shugo Tohyama,[1] Hisayuki Hashimoto,[1] Toru Egashira,[1] Yoko Tanimoto,[2] Saori Mizuno,[2] Shoma Tanaka,[3] Hironobu Okuno,[3] Kazuki Yamazawa,[4] Hideo Watanabe,[5] Mayumi Oda,[6] Ruri Kaneda,[1] Yumi Matsuzaki,[3] Toshihiro Nagai,[8] Hideyuki Okano,[3] Ken-ichi Yagami,[2] Mamoru Tanaka,[7] and Keiichi Fukuda[1]

[1]Department of Cardiology, Keio University School of Medicine, Shinjuku-ku, Tokyo 160-8582, Japan
[2]Laboratory Animal Resource Center, University of Tsukuba, Tsukuba, Ibaraki 305-8575, Japan
[3]Department of Physiology, Keio University School of Medicine, Tokyo 160-8582, Japan
[4]Department of Pediatrics, Keio University School of Medicine, Tokyo 160-8582, Japan
[5]Division of Pulmonary, Critical Care and Sleep Medicine, Departments of Medicine and Genetics and Genomic Sciences, Tisch Cancer Institute, Icahn School of Medicine at Mount Sinai, New York, NY 10029, USA
[6]Sakaguchi Laboratory, Department of Systems Medicine, Keio University School of Medicine, Tokyo 160-8582, Japan
[7]Department of Obstetrics and Gynecology, Keio University School of Medicine, Tokyo 160-8582, Japan
[8]Electron Microscope Laboratory, Keio University School of Medicine, Tokyo 160-8582, Japan
*Correspondence: yuasa@keio.jp
http://dx.doi.org/10.1016/j.stemcr.2016.04.015

SUMMARY

Embryonic stem cells (ESCs) are a hallmark of ideal pluripotent stem cells. Epigenetic reprogramming of induced pluripotent stem cells (iPSCs) has not been fully accomplished. iPSC generation is similar to somatic cell nuclear transfer (SCNT) in oocytes, and this procedure can be used to generate ESCs (SCNT-ESCs), which suggests the contribution of oocyte-specific constituents. Here, we show that the mammalian oocyte-specific linker histone *H1foo* has beneficial effects on iPSC generation. Induction of *H1foo* with *Oct4*, *Sox2*, and *Klf4* significantly enhanced the efficiency of iPSC generation. *H1foo* promoted in vitro differentiation characteristics with low heterogeneity in iPSCs. *H1foo* enhanced the generation of germline-competent chimeric mice from iPSCs in a manner similar to that for ESCs. These findings indicate that *H1foo* contributes to the generation of higher-quality iPSCs.

INTRODUCTION

Induced pluripotent stem cells (iPSCs) can be generated from somatic cells by introducing *Oct4*, *Sox2*, *Klf4*, and *c-Myc* (Takahashi and Yamanaka, 2006). This can be achieved by reprogramming the transcription network and epigenetic signature of the parental somatic cells. iPSCs have several benefits for basic research, drug innovation, and regeneration therapy. However, recent studies have reported genetic and epigenetic variations with iPSCs (Hussein et al., 2011; Kim et al., 2010; Polo et al., 2010; Ruiz et al., 2012; Stadtfeld et al., 2010; Taapken et al., 2011), which influences gene expression and could lead to functional diversity within iPSC replicates (Liang and Zhang, 2013). In fact, several studies have reported the heterogeneous differentiation potential among generated iPSC clones compared with those of embryonic stem cells (ESCs) (Feng et al., 2010; Hu et al., 2010; Narsinh et al., 2011). It is important that every iPSC clone shows high quality without variation for basic research and clinical purposes. Many attempts have been made to solve these problems by various methods (Gafni et al., 2013), but not all iPSCs exhibit quality as high as that of ESCs.

The reprogramming of somatic cells was originally demonstrated by producing cloned frogs using somatic cell nuclear transfer (SCNT) into *Xenopus* oocytes (Gurdon et al., 1958). Reprogramming of mammalian somatic cells has also been achieved using SCNT into oocytes, including those of mice and humans (Noggle et al., 2011; Wakayama et al., 1998). The procedure of SCNT into oocytes is similar to iPSC generation with respect to the time course of extinction of the parental gene-expression profile and activation of pluripotency (Egli et al., 2011). Both somatic cell reprogramming processes involve dynamic rearrangement of the epigenetic profile (Apostolou and Hochedlinger, 2013; Hussein et al., 2014). These findings suggest that the constituents of oocytes include a reprogramming-promoting factor. The linker histone H1 family binds to linker DNA and generates higher-order chromatin structures to control gene expression. Most members of the linker histone family consist of somatic linker histones that condense chromatin; therefore, these structures generally repress global gene-transcription activity (Hebbar and Archer, 2008; Steinbach et al., 1997). Mammalian oocytes contain the maternal-specific linker histone *H1foo*, a homolog of the *Xenopus* linker histone *B4*. *H1foo* is specifically expressed during the germinal vesicle stage and until the late two-cell or early four-cell stage, coincident with the early wave of zygotic genome reactivation (Gao et al., 2004; Tanaka et al., 2003, 2005). In *Xenopus* SCNT, somatic linker histones in transplanted nuclei are rapidly exchanged for linker histone *B4*, and the transplanted

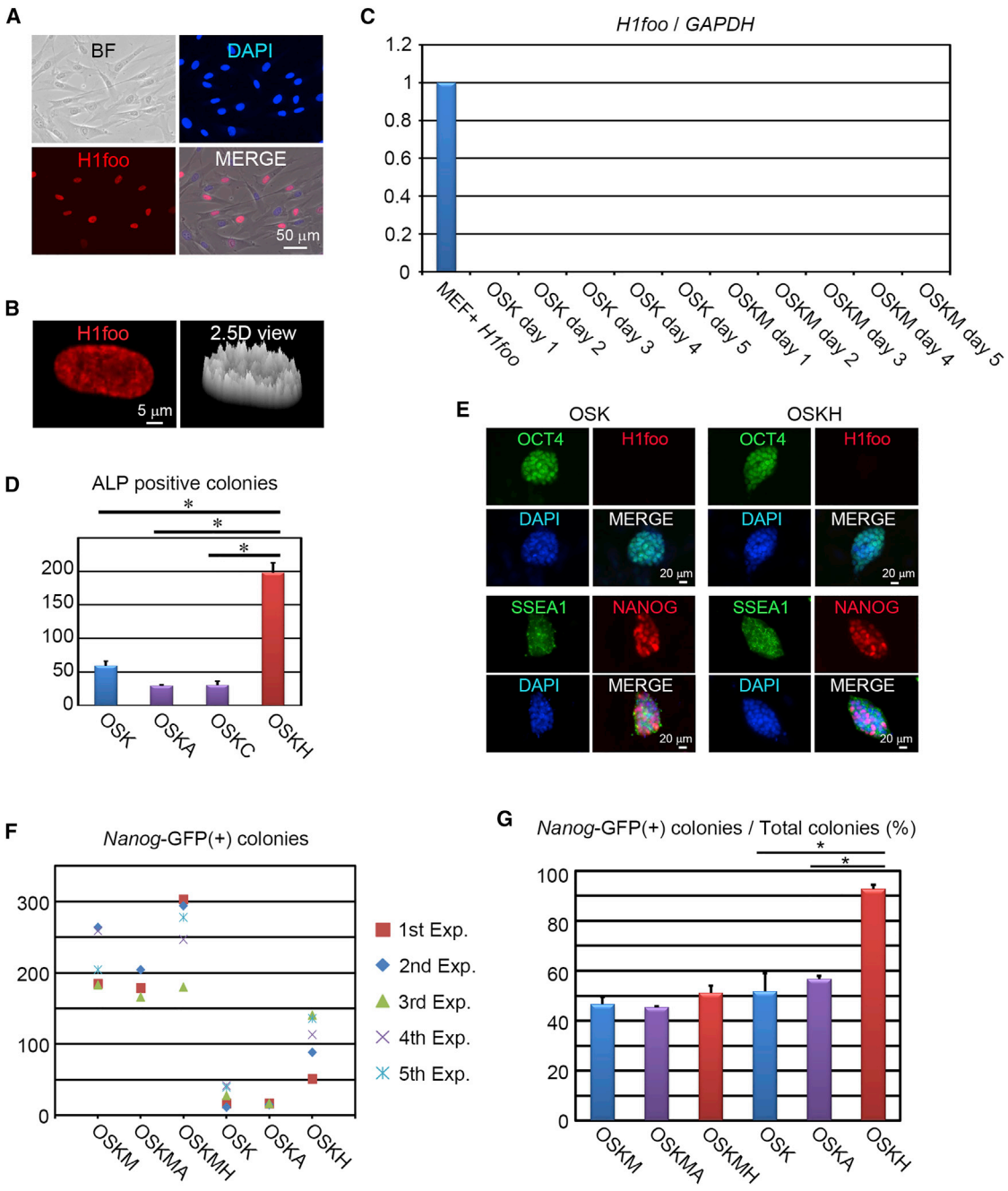

Figure 1. Exogenous Expression of *H1foo* Promotes iPSC Generation

(A) Immunostaining for H1foo (red), including nuclei stained with DAPI (blue) and bright-field (BF) images. Scale bar, 50 μm.

(B) Immunostaining for H1foo (red) with a 2D image (left) and a 2.5D image (right). The density of H1foo is depicted by the height in the 2.5D view. Scale bar, 5 μm.

(C) qRT-PCR analysis of endogenous *H1foo* expression during reprogramming, normalized by *H1foo* expression in *H1foo*-overexpressed MEFs (n = 3 independent experiments).

(D) Alkaline phosphatase-positive iPSC colony formations for OSK, OSK with *H1a* (OSK + *H1a*; OSKA), OSK with *H1c* (OSK + *H1c*; OSKC), and OSK with *H1foo* (OSK + *H1foo*; OSKH). Error bars represent the SEM (n = 3 independent experiments). *p < 0.05.

(legend continued on next page)

nuclei begin to swell and initiate decondensation (Byrne et al., 2003; Jullien et al., 2010); furthermore, in mouse SCNT the same phenomenon is observed with *H1foo* (Becker et al., 2005). Unlike other somatic linker histones, *B4* and *H1foo* do not restrict the accessibility of the linker DNA, but decondense the chromatin and permit transcriptional activation (Hayakawa et al., 2012; Saeki et al., 2005).

Based on these studies, we hypothesized that *H1foo* has a beneficial effect on iPSC generation. Here, we show that *H1foo* enhanced the generation of mouse iPSCs when co-expressed with *Oct4*, *Sox2*, and *Klf4*. Furthermore, *H1foo* promoted several in vitro differentiation characteristics with low heterogeneity in iPSCs that were similar to those of ESCs. Specifically, *H1foo* enhanced germline-competent chimeric mouse generation. These findings indicate that *H1foo* contributes to the generation of higher-quality iPSCs.

RESULTS

Exogenous Expression of *H1foo* Promotes Qualified iPSC Generation

We examined the effect of exogenous *H1foo* on somatic cell reprogramming by introducing *H1foo* during iPSC generation with *Oct4*, *Sox2*, and *Klf4* (OSK) or *Oct4*, *Sox2*, *Klf4*, and *c-Myc* (OSKM). Retrovirus vector-mediated exogenous *H1foo* was exclusively expressed in the nucleus of adult mouse tail-tip fibroblasts (Figures 1Aand S1A) and highly expressed peripherally in the nucleus (Figure 1B). SCNT into oocytes induced swelling of nuclei and chromatin decondensation (Gao et al., 2004; Tamada et al., 2006; Teranishi et al., 2004), so we investigated the effect of *H1foo* on nuclei (Figure S1B). We found that *H1a*, *H1c*, and *H1foo* had no significant effect on nuclear swelling (Figures S1C and S1D). However, interestingly, only *H1foo* reduced the intensively stained area, namely the heterochromatin area (Figure S1E). Next, we addressed whether intrinsic *H1foo* might be expressed during iPSC generation from mouse embryonic fibroblasts (MEFs) by introducing OSK or OSKM. However, we did not observe detectable intrinsic *H1foo* expression (Figure 1C). Co-expression of *H1foo* with OSK (OSKH) significantly enhanced the number of alkaline phosphatase-positive ESC-like colonies compared with OSK, OSK and *H1a* (OSKA), or OSK and *H1c* (OSKC) (Figure 1D). The OSKH-iPSCs expressed pluripotency markers similarly to control iPSCs (OSK), and *H1foo* was silenced (Figure 1E). We then examined the effect of *H1foo* on qualified iPSC generation using tail-tip fibroblasts from *Nanog*-GFP transgenic adult mice (Okita et al., 2007) (Figure S1G). Interestingly, *H1foo* also maximally promoted *Nanog*-GFP-positive colony generation (8-fold) during iPSC generation by OSK (Figure 1F). Notably, *H1foo* specifically enhanced GFP-positive colonies as opposed to GFP-negative colonies (Figure 1G).

Characteristics of OSKH-iPSC Generation

Next, we examined the iPSC characteristics produced by OSK and OSKH. The OSKH-iPSCs expressed pluripotency markers similar to those of OSK-iPSCs. Meanwhile the transgenes, including *H1foo*, were silenced (Figure 2A). Regarding the growth rate of iPSCs, there was no significant difference between OSK- and OSKH-treated cells (Figure S1F). We investigated the differences in global gene-transcriptome profiles among ESCs, three replicates of OSK-iPSCs, and four replicates of OSKH-iPSCs. All cell types were remarkably similar and showed a correlation coefficient (R^2) of 0.99 (Figures 2B and 2C). We then examined DNA demethylation in the promoter regions of pluripotency marker genes (Figure S1H) and the differentiation potencies by teratoma formation (Figure S1I). Furthermore, we focused on genes differentially expressed between OSK-iPSCs and OSKH-iPSCs. We chose eight differentially expressed genes, which were statistically significant with more than a 2-fold difference between OSK-iPSCs and OSKH-iPSCs ($p < 0.05$). Many of the genes showed more similar expression patterns between OSKH-iPSCs and ESCs than between OSK-iPSCs and ESCs (Figures S2A–S2H), but the expression levels of these transcripts were heterogeneous among the replicates in the same cell type, indicating that those genes would not have a definitive role in stem cell properties. Although a definitive marker that reflects the quality of iPSCs has not been found, aberrant epigenetic silencing of the *Dlk1-Dio3* gene cluster could indicate developmental potency, particularly because it contributes to the ratio of chimerism in mouse iPSCs (Stadtfeld et al., 2010). We analyzed the methylation status of an intergenic differentially methylated region (*IG*-DMR) that is located between the *Dlk1* and *Gtl2* genes and a *Gtl2* differentially methylated region (*Gtl2*-DMR) (Figures 2D and 2E). Both loci in OSKH-iPSCs were highly demethylated, similarly to ESCs and MEFs. We next investigated the expression of several transcripts that increase or diminish in the early reprogramming phase (Lujan et al., 2015). Interestingly, OSKH-induced MEFs showed significant upregulation of several early reprogramming

(E) Immunostaining for pluripotency markers (OCT4 [green], SSEA1 [green], and Nanog [red]), including *H1foo* (red) and nuclei stained with DAPI (blue) in OSK-iPSCs and OSKH-iPSCs. Scale bars, 20 μm.

(F) Number of *Nanog*-GFP-positive iPSC colonies in each experiment (n = 5 independent experiments).

(G) Proportion of *Nanog*-GFP-positive colonies to the total number of ESC-like colonies. Error bars represent the SEM (n = 5 independent experiments). *$p < 0.05$.

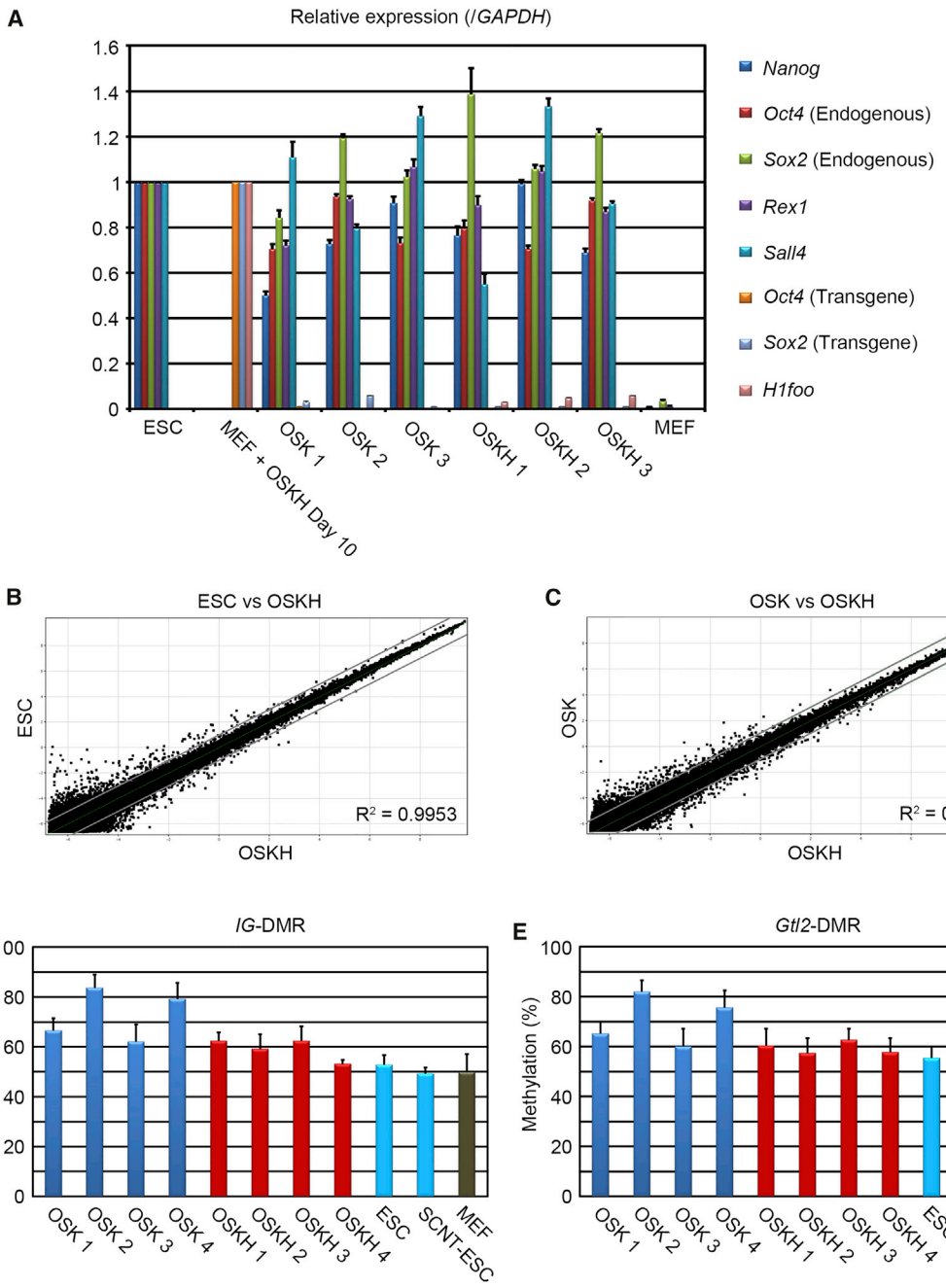

Figure 2. Characteristics of OSKH-Induced iPSCs

(A) qRT-PCR analysis of pluripotency genes and *H1foo* in iPSCs. Error bars represent the SEM (n = 3 independent experiments).

(B and C) Pairwise scatterplots of global gene-expression cDNA microarray patterns of OSKH-iPSCs (n = 4) compared with ESC (n = 1) (B) or OSK-iPSCs (n = 3) (C). The gray lines indicate $\log_2$ 2-fold changes in gene-expression levels between the paired cell types.

(D and E) Degree of DNA methylation at IG-DMR and Gtl2-DMR in four OSK iPSC clones, four OSKH-iPSC clones, and ESCs, as well as MEFs analyzed by pyrosequencing. Error bars represent the SEM (n = 3 independent experiments).

markers (Figures S2I, S2J, and S2K) and downregulation of fibroblast markers (Figures S2L and S2M) in comparison with OSK- or OSKA-induced MEFs. We confirmed that OSKH correctly traces the same pathway already reported.

H1foo Enhances the In Vitro Differentiation Potential

Next, we asked whether *H1foo* could improve the quality of iPSCs. Often iPSCs highly express pluripotency markers but show poor differentiation efficiency in vitro, including

characteristics such as a low number of embryoid bodies (EBs) and frazzled EBs with poor differentiation potential. Moreover, this undesired trend is highly apparent in low-passage iPSCs and is correlated to the remnant source cell epigenetic memories (Kim et al., 2010; Polo et al., 2010). We examined the differentiation potency by EB formation in low-passage (P5) OSK-iPSCs, OSKH-iPSCs, and two types of ESCs as controls. First, we examined the number and the size of EBs at 5 days after differentiation (Figure S3A), which were more similar between OSKH-iPSCs and ESCs than between OSK-iPSCs and ESCs (Figures 3A and 3B). Furthermore, the variance of EB size was smaller in OSKH-iPSCs than in OSK-iPSCs (Figures 3C and 3D). OSKH-iPSCs expressed a higher content of proliferation markers than OSK-iPSCs (Figures 3E and 3F). However, a significant difference was not observed in the differentiation marker profiles among ESCs, OSK-iPSCs, and OSKH-iPSCs (Figure S3B). We also examined the population of apoptotic cells during differentiation. Apoptosis in OSKH-iPSCs was suppressed compared with OSK-iPSCs (Figures 3G and S3C). Taken together, the data suggest that *H1foo* causes iPSCs to be more adaptable to in vitro differentiation conditions and promotes the homogeneity of EBs.

H1foo Enhances the In Vivo Differentiation Potential

We finally investigated the in vivo differentiation potential of OSK-iPSCs and OSKH-iPSCs using a co-culture aggregation method (Eakin and Hadjantonakis, 2006). First we examined the chromosome number, which showed no significant difference in chromosomal abnormality between OSK-iPSCs and OSKH-iPSCs (Figure 4A). Each iPSC clone was aggregated with 100 ICR mouse embryos at the eight-cell stage, and chimeric embryos were transferred into the uteri of pseudopregnant females. Notably, OSKH-iPSCs generated more live chimeras, with higher chimerism, than OSK-iPSCs (Figures 4B, 4C, S4B, and S4C). Moreover, some OSKH-iPSC clones generated more 100% chimeras than ESCs (Figure S4B). Germline transmission potential is one of the most stringent hallmarks of pluripotent stem cells. We examined the germline transmission from 100% chimeric mice by in vitro fertilization. OSKH-iPSCs generated many pups with colored coats, confirming the favorable germline transmission potential of OSKH-iPSCs (Figures 4E, S4D, and S4E). We did not find any phenotypic abnormalities in these pups.

DISCUSSION

H1foo promoted the generation of *Nanog*-GFP-positive colonies when it was co-expressed with OSK. Notably, the proportion of GFP-positive colonies was improved to 90%. OSKH-iPSCs demonstrated differentiation potency more similar to that of ESCs than did OSK-iPSCs, especially with respect to in vitro EB formation, chimerism, and germline transmission in vivo. We also examined the effect of *H1foo* with *Oct4*, *Sox2*, *Klf4*, and *c-Myc*, but the number of alkaline phosphatase-positive colonies and *Nanog*-GFP colonies, and the proportion of GFP-positive colonies were not significantly different to those of OSKM-iPSCs. *c-Myc* promotes iPSC generation but is not essential for reprogramming. On the other hand, *c-Myc* lowers the proportion of *Nanog*-GFP-positive colonies and increases the tumorigenicity of cells (Nakagawa et al., 2008). Therefore, it is preferable to omit *c-Myc* in iPSC generation, although it is still commonly used to promote reprogramming efficiency. We showed here that *H1foo* could be substituted for *c-Myc* in terms of reprogramming efficiency and showed superiority with respect to qualifying iPSCs.

Recent studies have demonstrated that oocyte constituents play a key role in somatic cell reprogramming in SCNT. Co-expression of maternal-specific factors in oocytes, such as Glis1 (Maekawa et al., 2011) and TH2A/TH2B (Shinagawa et al., 2014), enhances the reprogramming efficiency of iPSC generation. Investigation of maternal-specific factors in oocytes has great potential for innovating somatic cell reprogramming and deciphering the reprogramming mechanisms (Gurdon and Wilmut, 2011). *H1foo* is specifically expressed during the germinal vesicle stage and is essential for oocyte maturation (Furuya et al., 2007; Gao et al., 2004). Interestingly, exogenous expression of *H1foo* in ESCs leads to the prevention of differentiation in vitro due to continuous pluripotency gene activation (Hayakawa et al., 2012). In our study, *H1foo* was properly silenced in generated iPSCs, which induced successful reprogramming but did not hinder the differentiation potency of OSKH-iPSCs.

The detailed molecular mechanisms regarding how *H1foo* enhances the reprogramming efficiency in iPSC generation and why OSKH-iPSCs exhibit improved quality remain elusive. The higher-order chromatin structure is crucially dependent on architectural chromatin proteins, including the family of linker histone proteins. Although somatic cells contain numerous linker histone variants, only one, *H1foo*, is present in mouse oocytes (Tanaka et al., 2001). In the mouse egg, somatic linker histones in sperm-derived chromatin are rapidly replaced by H1foo after fertilization (Tanaka et al., 2001). In SCNT oocytes, the somatic linker histone H1c in the donor chromatin is also rapidly replaced by H1foo in mice (Gao et al., 2004; Teranishi et al., 2004). In *Xenopus* SCNT, oocyte-specific linker histone B4 loading to genome-wide somatic chromatin is required for successful reprogramming (Jullien et al., 2010, 2014; Miyamoto et al., 2007). In the early phase of the reprogramming process, global loss of histone H3 lysine 27 trimethylation (H3K27me3) occurs and epigenetic modification affects

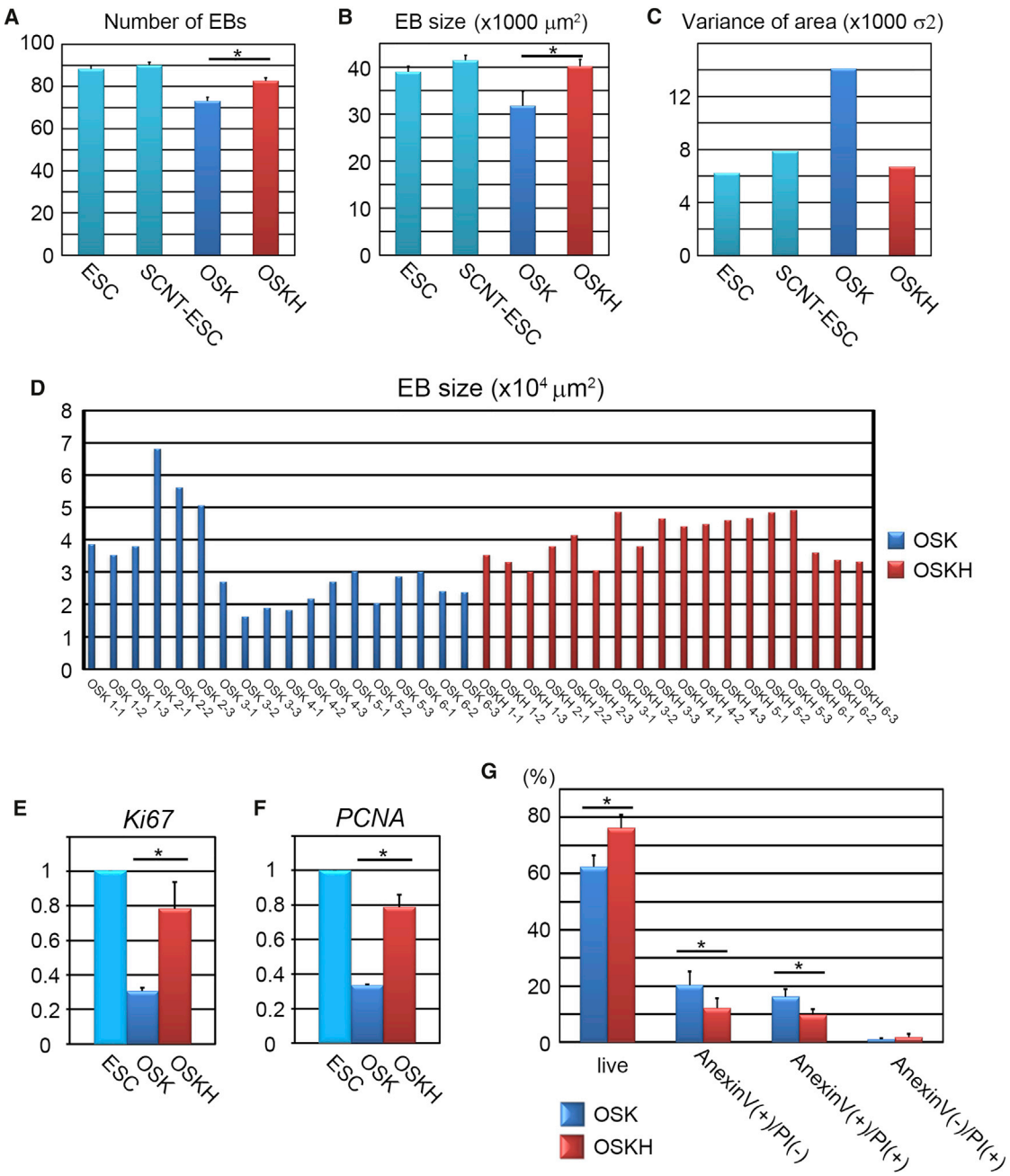

Figure 3. In Vitro Differentiation Potential in OSKH-iPSCs

(A) Number of EBs on day 5 after differentiation. Error bars represent the SEM (n = 3 independent experiments). *p < 0.05.

(B) Size of EBs on day 5 after differentiation. Error bars represent the SEM (n = 3 independent experiments). *p < 0.05.

(C) Variance of EB sizes from each ESCs and iPSCs (n = 3 independent experiments).

(D) Variation of EB sizes. Each bar represents one experiment.

(E and F) Cell-proliferation markers Ki67 (E) and proliferating cell nuclear antigen (PCNA; F) on day 2 after differentiation. Error bars represent the SEM (n = 3 independent experiments). *p < 0.05.

(G) Apoptotic cell distribution determined by fluorescence-activated cell sorting analysis of cells labeled with annexin V-fluorescein isothiocyanate and propidium iodide (PI) on day 1 after differentiation induction. Error bars represent the SEM (n = 3 independent experiments). *p < 0.05.

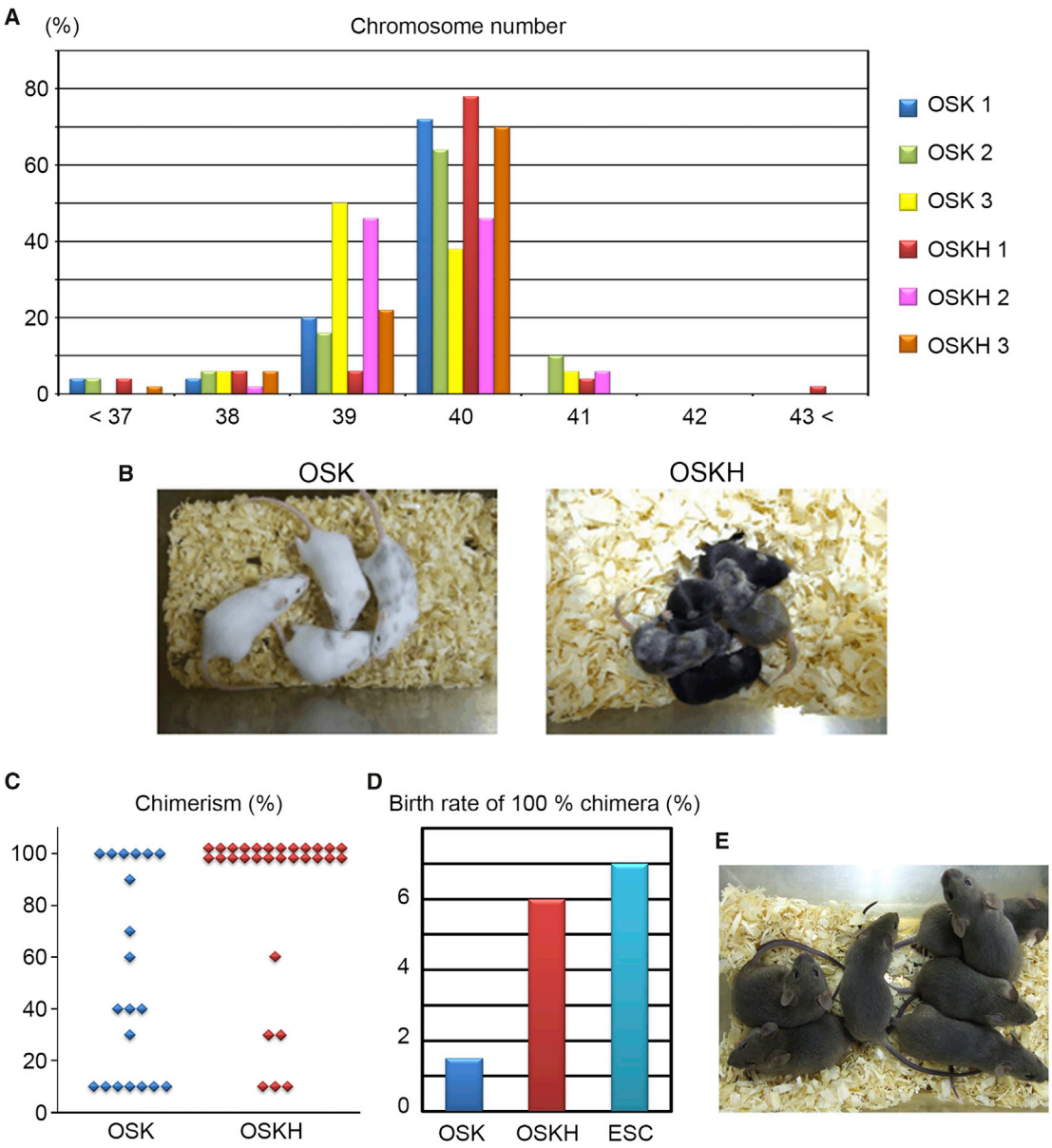

Figure 4. In Vivo Differentiation Potential in OSKH-iPSCs

(A) Chromosome number of each iPSC.

(B) Chimeric mice generated from OSK-iPSCs or OSKH-iPSCs.

(C) Number of agouti coat colored chimeric mice derived from each of four replicates of iPSCs.

(D) Birth rate of 100% chimeric mice (100% chimeric mice/embryos transferred).

(E) The coat color of pups from a 100% chimeric OSKH mouse shows germline transmission.

the status of heterochromatin (Hussein et al., 2014). In our study, *H1foo* reduced the heterochromatin area, which is consistent with previous reports that *H1foo* keeps chromatin looser than somatic H1 and other linker histones, and may support the generation of a more suitable chromatin state for reprogramming. These data suggest that dominant occupancy of oocyte-specific linker histone in donor chromatin may be required for successful reprogramming and might erase the parental epigenetic status. To determine whether innate *H1foo* would cooperatively induce reprogramming during iPSC generation by OSK, we examined *H1foo* expression during iPSC generation by OSK. We did not detect *H1foo* expression, which suggests that *H1foo* is not essential for OSK-dependent reprogramming. Therefore, we did not perform loss-of-function experiments such as *H1foo* knockdown by small interfering RNA.

H1foo induced successful reprogramming for iPSC generation in a stringent assay, thus contributing to chimerism and germline transmission. Although in vivo experiments cannot be performed in humans, it is important to generate high-quality iPSCs without variation among different iPSC lines.

EXPERIMENTAL PROCEDURES

Details of all procedures are available in Supplemental Experimental Procedures.

All experiments were performed in accordance with the Keio University Animal Care Guidelines and were approved by the Ethics Committee of Keio University (20-041-4), which conforms to the Guide for the Care and Use of Laboratory Animals published by the US National Institutes of Health.

ACCESSION NUMBERS

The accession number for the microarray data reported in this paper is GEO: GSE79515.

SUPPLEMENTAL INFORMATION

Supplemental Information includes Supplemental Experimental Procedures, four figures, and one table and can be found with this article online at http://dx.doi.org/10.1016/j.stemcr.2016.04.015.

AUTHOR CONTRIBUTIONS

S.Y. designed the research. A.K., S.Y., F.S., Y.S., T.S., D.K., S.K., M.T., S.T., H.H., T.E., Y.T., S.M., S.T., H.O., K.Y., H.W., M.O., and R.K. performed the research. T.N. conducted the electron microscopic observation. A.K., S.Y., F.S., Y.M., H.O., K.Y., M.T., and K.F. analyzed the data. A.K. and S.Y. wrote the paper.

ACKNOWLEDGMENTS

Nanog-GFP-IRES-puro transgenic mice were kindly provided from Dr. Shinya Yamanaka. Several ESCs were kindly donated: R1 ESC from Dr. John C. Roder, B6J-23$^{-(UTR)}$ ESC from Dr. Fumihiro Sugiyama, and SCNT-ESC (B6mt-1) from Riken BioResource Center. This study was supported in part by research grants from Grants-in-Aid for Scientific Research (JSPS KAKENHI grant numbers 24117716, 26670408, 15H01521, 15K14431), the Highway Program for Realization of Regenerative Medicine from Japan Science and Technology Agency, the Program for Intractable Diseases Research utilizing Disease-specific iPSCs from the Japan Agency For Medical Research and Development (AMED), Translational Research Network Program from AMED, and Keio University Medical Science Fund. H.O. is a Founding Scientist and a paid SAB of San Bio Co. Ltd.

Received: April 28, 2015
Revised: April 27, 2016
Accepted: April 28, 2016
Published: May 26, 2016

REFERENCES

Apostolou, E., and Hochedlinger, K. (2013). Chromatin dynamics during cellular reprogramming. Nature *502*, 462–471.

Becker, M., Becker, A., Miyara, F., Han, Z., Kihara, M., Brown, D.T., Hager, G.L., Latham, K., Adashi, E.Y., and Misteli, T. (2005). Differential in vivo binding dynamics of somatic and oocyte-specific linker histones in oocytes and during ES cell nuclear transfer. Mol. Biol. Cell *16*, 3887–3895.

Byrne, J.A., Simonsson, S., Western, P.S., and Gurdon, J.B. (2003). Nuclei of adult mammalian somatic cells are directly reprogrammed to oct-4 stem cell gene expression by amphibian oocytes. Curr. Biol. *13*, 1206–1213.

Eakin, G.S., and Hadjantonakis, A.-K. (2006). Production of chimeras by aggregation of embryonic stem cells with diploid or tetraploid mouse embryos. Nat. Protoc. *1*, 1145–1153.

Egli, D., Chen, A.E., Saphier, G., Ichida, J., Fitzgerald, C., Go, K.J., Acevedo, N., Patel, J., Baetscher, M., Kearns, W.G., et al. (2011). Reprogramming within hours following nuclear transfer into mouse but not human zygotes. Nat. Commun. *2*, 488.

Feng, Q., Lu, S.J., Klimanskaya, I., Gomes, I., Kim, D., Chung, Y., Honig, G.R., Kim, K.S., and Lanza, R. (2010). Hemangioblastic derivatives from human induced pluripotent stem cells exhibit limited expansion and early senescence. Stem Cells *28*, 704–712.

Furuya, M., Tanaka, M., Teranishi, T., Matsumoto, K., Hosoi, Y., Saeki, K., Ishimoto, H., Minegishi, K., Iritani, A., and Yoshimura, Y. (2007). H1foo is indispensable for meiotic maturation of the mouse oocyte. J. Reprod. Dev. *53*, 895–902.

Gafni, O., Weinberger, L., Mansour, A.A., Manor, Y.S., Chomsky, E., Ben-Yosef, D., Kalma, Y., Viukov, S., Maza, I., Zviran, A., et al. (2013). Derivation of novel human ground state naive pluripotent stem cells. Nature *504*, 282–286.

Gao, S., Chung, Y.G., Parseghian, M.H., King, G.J., Adashi, E.Y., and Latham, K.E. (2004). Rapid H1 linker histone transitions following fertilization or somatic cell nuclear transfer: evidence for a uniform developmental program in mice. Dev. Biol. *266*, 62–75.

Gurdon, J.B., and Wilmut, I. (2011). Nuclear transfer to eggs and oocytes. Cold Spring Harbor Perspect. Biol. *3*. http://dx.doi.org/10.1101/cshperspect.a002659.

Gurdon, J.B., Elsdale, T.R., and Fischberg, M. (1958). Sexually mature individuals of *Xenopus laevis* from the transplantation of single somatic nuclei. Nature *182*, 64–65.

Hayakawa, K., Ohgane, J., Tanaka, S., Yagi, S., and Shiota, K. (2012). Oocyte-specific linker histone H1foo is an epigenomic modulator that decondenses chromatin and impairs pluripotency. Epigenetics *7*, 1029–1036.

Hebbar, P.B., and Archer, T.K. (2008). Altered histone H1 stoichiometry and an absence of nucleosome positioning on transfected DNA. J. Biol. Chem. *283*, 4595–4601.

Hu, B.Y., Weick, J.P., Yu, J., Ma, L.X., Zhang, X.Q., Thomson, J.A., and Zhang, S.C. (2010). Neural differentiation of human induced pluripotent stem cells follows developmental principles but with variable potency. Proc. Natl. Acad. Sci. USA *107*, 4335–4340.

Hussein, S.M., Batada, N.N., Vuoristo, S., Ching, R.W., Autio, R., Narva, E., Ng, S., Sourour, M., Hamalainen, R., Olsson, C., et al.

(2011). Copy number variation and selection during reprogramming to pluripotency. Nature *471*, 58–62.

Hussein, S.M., Puri, M.C., Tonge, P.D., Benevento, M., Corso, A.J., Clancy, J.L., Mosbergen, R., Li, M., Lee, D.S., Cloonan, N., et al. (2014). Genome-wide characterization of the routes to pluripotency. Nature *516*, 198–206.

Jullien, J., Astrand, C., Halley-Stott, R.P., Garrett, N., and Gurdon, J.B. (2010). Characterization of somatic cell nuclear reprogramming by oocytes in which a linker histone is required for pluripotency gene reactivation. Proc. Natl. Acad. Sci. USA *107*, 5483–5488.

Jullien, J., Miyamoto, K., Pasque, V., Allen, G.E., Bradshaw, C.R., Garrett, N.J., Halley-Stott, R.P., Kimura, H., Ohsumi, K., and Gurdon, J.B. (2014). Hierarchical molecular events driven by oocyte-specific factors lead to rapid and extensive reprogramming. Mol. Cell *55*, 524–536.

Kim, K., Doi, A., Wen, B., Ng, K., Zhao, R., Cahan, P., Kim, J., Aryee, M.J., Ji, H., Ehrlich, L.I., et al. (2010). Epigenetic memory in induced pluripotent stem cells. Nature *467*, 285–290.

Liang, G., and Zhang, Y. (2013). Genetic and epigenetic variations in iPSCs: potential causes and implications for application. Cell Stem Cell *13*, 149–159.

Lujan, E., Zunder, E.R., Ng, Y.H., Goronzy, I.N., Nolan, G.P., and Wernig, M. (2015). Early reprogramming regulators identified by prospective isolation and mass cytometry. Nature *521*, 352–356.

Maekawa, M., Yamaguchi, K., Nakamura, T., Shibukawa, R., Kodanaka, I., Ichisaka, T., Kawamura, Y., Mochizuki, H., Goshima, N., and Yamanaka, S. (2011). Direct reprogramming of somatic cells is promoted by maternal transcription factor Glis1. Nature *474*, 225–229.

Miyamoto, K., Furusawa, T., Ohnuki, M., Goel, S., Tokunaga, T., Minami, N., Yamada, M., Ohsumi, K., and Imai, H. (2007). Reprogramming events of mammalian somatic cells induced by *Xenopus laevis* egg extracts. Mol. Reprod. Dev. *74*, 1268–1277.

Nakagawa, M., Koyanagi, M., Tanabe, K., Takahashi, K., Ichisaka, T., Aoi, T., Okita, K., Mochiduki, Y., Takizawa, N., and Yamanaka, S. (2008). Generation of induced pluripotent stem cells without Myc from mouse and human fibroblasts. Nat. Biotechnol. *26*, 101–106.

Narsinh, K.H., Sun, N., Sanchez-Freire, V., Lee, A.S., Almeida, P., Hu, S., Jan, T., Wilson, K.D., Leong, D., Rosenberg, J., et al. (2011). Single cell transcriptional profiling reveals heterogeneity of human induced pluripotent stem cells. J. Clin. Invest. *121*, 1217–1221.

Noggle, S., Fung, H.L., Gore, A., Martinez, H., Satriani, K.C., Prosser, R., Oum, K., Paull, D., Druckenmiller, S., Freeby, M., et al. (2011). Human oocytes reprogram somatic cells to a pluripotent state. Nature *478*, 70–75.

Okita, K., Ichisaka, T., and Yamanaka, S. (2007). Generation of germline-competent induced pluripotent stem cells. Nature *448*, 313–317.

Polo, J.M., Liu, S., Figueroa, M.E., Kulalert, W., Eminli, S., Tan, K.Y., Apostolou, E., Stadtfeld, M., Li, Y., Shioda, T., et al. (2010). Cell type of origin influences the molecular and functional properties of mouse induced pluripotent stem cells. Nat. Biotechnol. *28*, 848–855.

Ruiz, S., Diep, D., Gore, A., Panopoulos, A.D., Montserrat, N., Plongthongkum, N., Kumar, S., Fung, H.L., Giorgetti, A., Bilic, J., et al. (2012). Identification of a specific reprogramming-associated epigenetic signature in human induced pluripotent stem cells. Proc. Natl. Acad. Sci. USA *109*, 16196–16201.

Saeki, H., Ohsumi, K., Aihara, H., Ito, T., Hirose, S., Ura, K., and Kaneda, Y. (2005). Linker histone variants control chromatin dynamics during early embryogenesis. Proc. Natl. Acad. Sci. USA *102*, 5697–5702.

Shinagawa, T., Takagi, T., Tsukamoto, D., Tomaru, C., Huynh, L.M., Sivaraman, P., Kumarevel, T., Inoue, K., Nakato, R., Katou, Y., et al. (2014). Histone variants enriched in oocytes enhance reprogramming to induced pluripotent stem cells. Cell Stem Cell *14*, 217–227.

Stadtfeld, M., Apostolou, E., Akutsu, H., Fukuda, A., Follett, P., Natesan, S., Kono, T., Shioda, T., and Hochedlinger, K. (2010). Aberrant silencing of imprinted genes on chromosome 12qF1 in mouse induced pluripotent stem cells. Nature *465*, 175–181.

Steinbach, O.C., Wolffe, A.P., and Rupp, R.A. (1997). Somatic linker histones cause loss of mesodermal competence in *Xenopus*. Nature *389*, 395–399.

Taapken, S.M., Nisler, B.S., Newton, M.A., Sampsell-Barron, T.L., Leonhard, K.A., McIntire, E.M., and Montgomery, K.D. (2011). Karotypic abnormalities in human induced pluripotent stem cells and embryonic stem cells. Nat. Biotechnol. *29*, 313–314.

Takahashi, K., and Yamanaka, S. (2006). Induction of pluripotent stem cells from mouse embryonic and adult fibroblast cultures by defined factors. Cell *126*, 663–676.

Tamada, H., Van Thuan, N., Reed, P., Nelson, D., Katoku-Kikyo, N., Wudel, J., Wakayama, T., and Kikyo, N. (2006). Chromatin decondensation and nuclear reprogramming by nucleoplasmin. Mol. Cell Biol. *26*, 1259–1271.

Tanaka, M., Hennebold, J.D., Macfarlane, J., and Adashi, E.Y. (2001). A mammalian oocyte-specific linker histone gene H1oo: homology with the genes for the oocyte-specific cleavage stage histone (cs-H1) of sea urchin and the B4/H1M histone of the frog. Development *128*, 655–664.

Tanaka, M., Kihara, M., Meczekalski, B., King, G.J., and Adashi, E.Y. (2003). H1oo: a pre-embryonic H1 linker histone in search of a function. Mol. Cell Endocrinol. *202*, 5–9.

Tanaka, M., Kihara, M., Hennebold, J.D., Eppig, J.J., Viveiros, M.M., Emery, B.R., Carrell, D.T., Kirkman, N.J., Meczekalski, B., Zhou, J., et al. (2005). H1FOO is coupled to the initiation of oocytic growth. Biol. Reprod. *72*, 135–142.

Teranishi, T., Tanaka, M., Kimoto, S., Ono, Y., Miyakoshi, K., Kono, T., and Yoshimura, Y. (2004). Rapid replacement of somatic linker histones with the oocyte-specific linker histone H1foo in nuclear transfer. Dev. Biol. *266*, 76–86.

Wakayama, T., Perry, A.C.F., Zuccotti, M., Johnson, K.R., and Yanagimachi, R. (1998). Full-term development of mice from enucleated oocytes injected with cumulus cell nuclei. Nature *394*, 369–374.

Stem Cell Reports, Volume *6*

Supplemental Information

H1foo Has a Pivotal Role in Qualifying Induced Pluripotent Stem Cells

Akira Kunitomi, Shinsuke Yuasa, Fumihiro Sugiyama, Yuki Saito, Tomohisa Seki, Dai Kusumoto, Shin Kashimura, Makoto Takei, Shugo Tohyama, Hisayuki Hashimoto, Toru Egashira, Yoko Tanimoto, Saori Mizuno, Shoma Tanaka, Hironobu Okuno, Kazuki Yamazawa, Hideo Watanabe, Mayumi Oda, Ruri Kaneda, Yumi Matsuzaki, Toshihiro Nagai, Hideyuki Okano, Ken-ichi Yagami, Mamoru Tanaka, and Keiichi Fukuda

Supplemental Figures

Figure S1 (Related to Figure 1). Characteristics of *H1foo* overexpressed fibroblasts and OSKH-induced iPSC generation

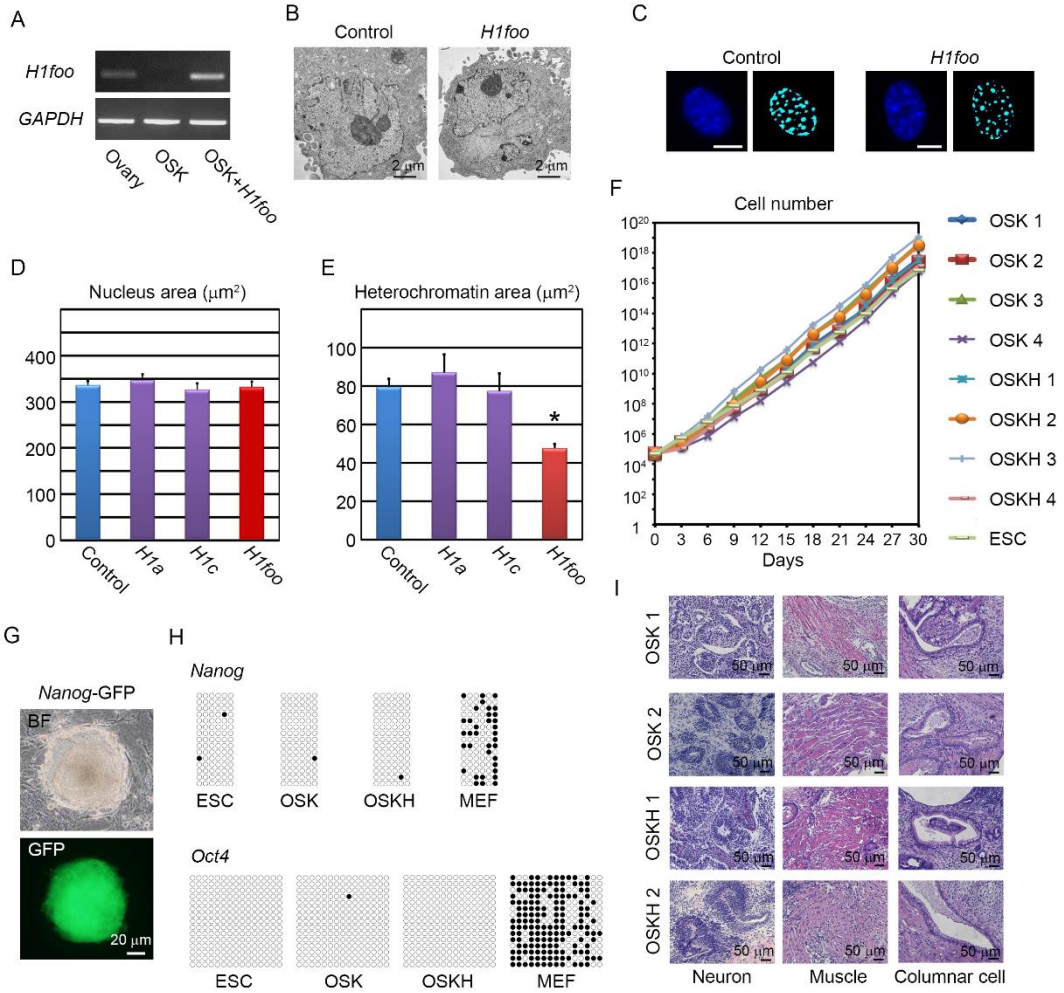

(A) RT-PCR analysis of *H1foo* in the ovaries, OSK-overexpressed fibroblasts, and OSKH-overexpressed fibroblasts. (B) Electron microscope image of control and *H1foo* overexpressed-fibroblasts. Scale bar, 2 μm. (C) Nuclei stained with DAPI of control and H1foo overexpressed fibroblasts (left side), DAPI intense stained heterochromatin domains (right side). Scale bar, 50 μm. (D) Nucleus area of control, *H1a*, *H1c* and *H1foo* overexpressed fibroblasts Error bars represent the SEM (n=4 independent experiments, 25 nuclei per experiment). *P<0.05. (E) DAPI intense stained heterochromatin domains of control, *H1a*, *H1c* and *H1foo* overexpressed fibroblasts Error bars represent the SEM (n=4 independent experiments, 25 nuclei per experiment). *P<0.05. (F) Cell growth of each iPSC. (G) *Nanog*-GFP positive iPSC colony from adult mouse tale-tip fibroblasts. Scale bar, 20 μm. (H) Bisulfite genomic sequencing of the promoter regions of *Nanog* and *Oct4* in ESCs, OSK-iPSCs, OSKH-iPSCs, and MEFs. Open circles indicate unmethylated CpG dinucleotides, and filled circles indicate methylated CpG dinucleotides (n=3 independent experiments). (I) Teratoma formation from each iPSC. Scale bar, 50 μm.

Figure S2 (Related to Figure 2). Quantitative RT-PCR analysis of differentially expressed genes among ESCs, OSK-iPSCs and OSKH-iPSCs. Quantitative RT-PCR analysis of early reprogramming markers and source cell markers.

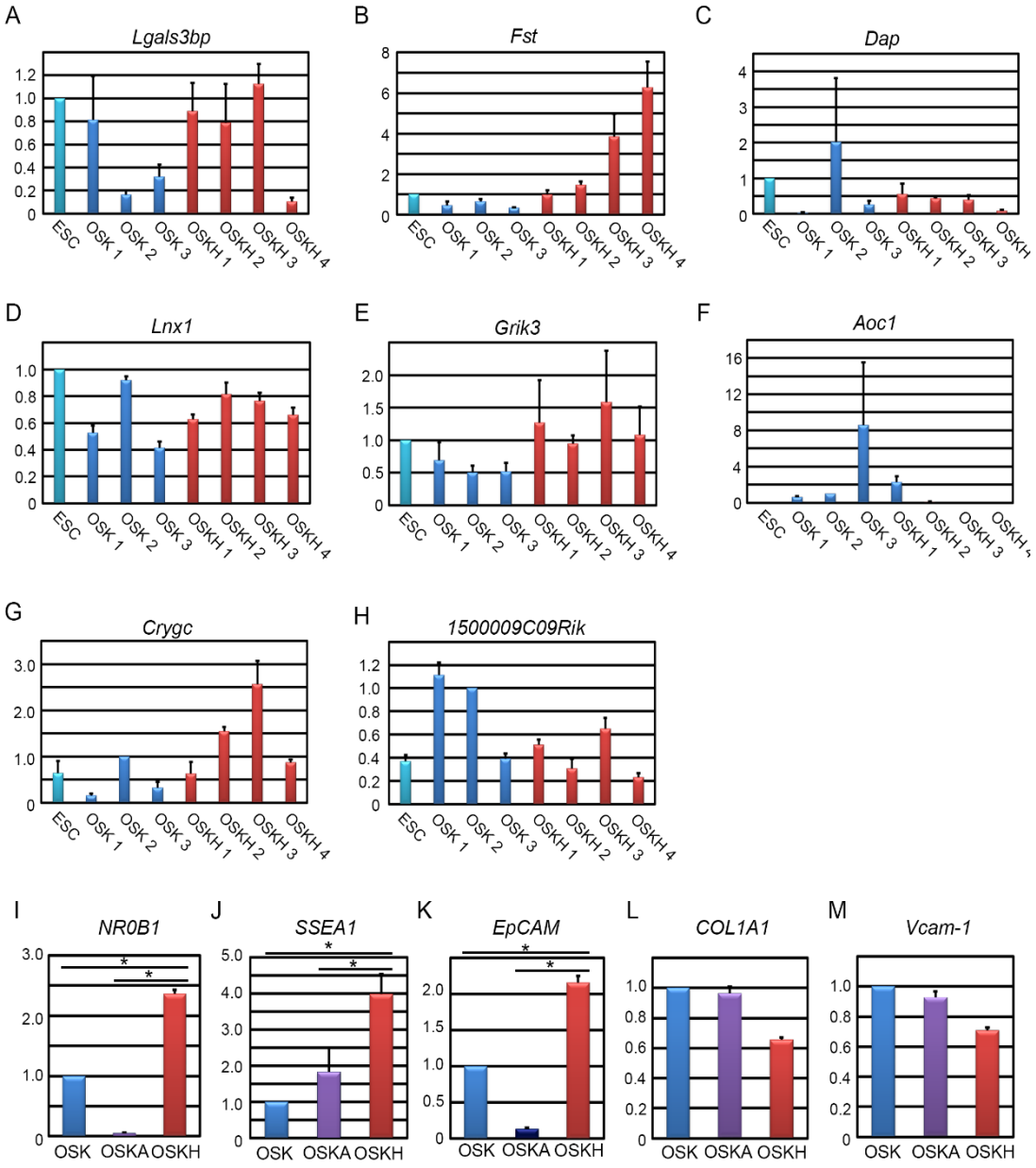

(A-H) Quantitative RT-PCR analysis of differentially expressed genes between OSK-iPSCs and OSKH-iPSCs. Error bars represent the SEM (n=3 independent experiments). *P<0.05. (I-K) Quantitative RT-PCR analysis of early reprogramming markers on day 5 after induction of reprogramming factors. Error bars represent the SEM (n=3 independent experiments). *P<0.05. (L, M) Quantitative RT-PCR analysis of fibroblast markers on day 5 after induction of reprogramming factors. Error bars represent the SEM (n=3 independent experiments).

Figure S3 (Related to Figure 3). Characteristics of embryoid bodies generated from OSK-iPSCs and OSKH-iPSCs.

A

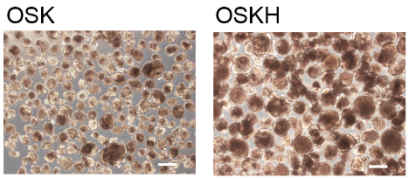

B

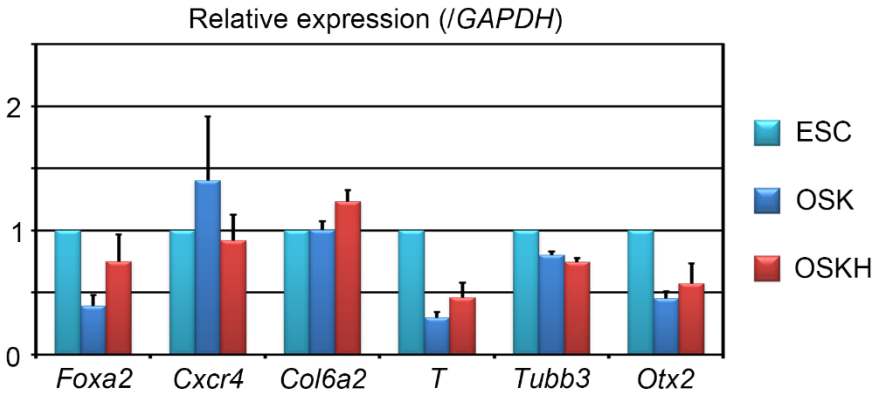

C

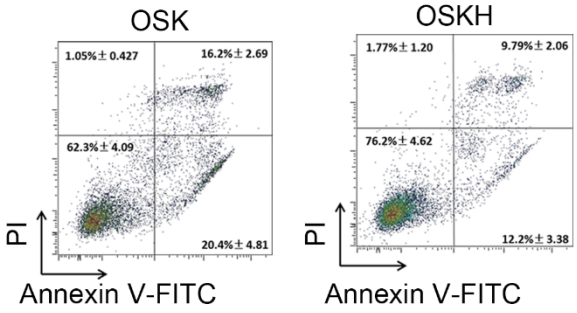

(A) EBs from each iPSC on day 5 after differentiation. Scale bar, 300 μm.

(B) The expression of endodermal markers (*Foxa2* and *Cxcr4*), mesodermal markers (*Col6a2* and *T*), and ectodermal markers (*Tubb3* and *Otx2*) was examined in ESCs and each iPSC on day 2 after differentiation. Error bars represent the SEM (n=3 independent experiments).

(C) Apoptotic cell distribution determined by FACS analysis of cells labeled with annexin V-FITC and propidium iodide (PI) on day 1 after differentiation induction (n=3 independent experiments).

Figure S4 (Related to Figure 4). Chimeric mouse generation from ESCs and iPSCs

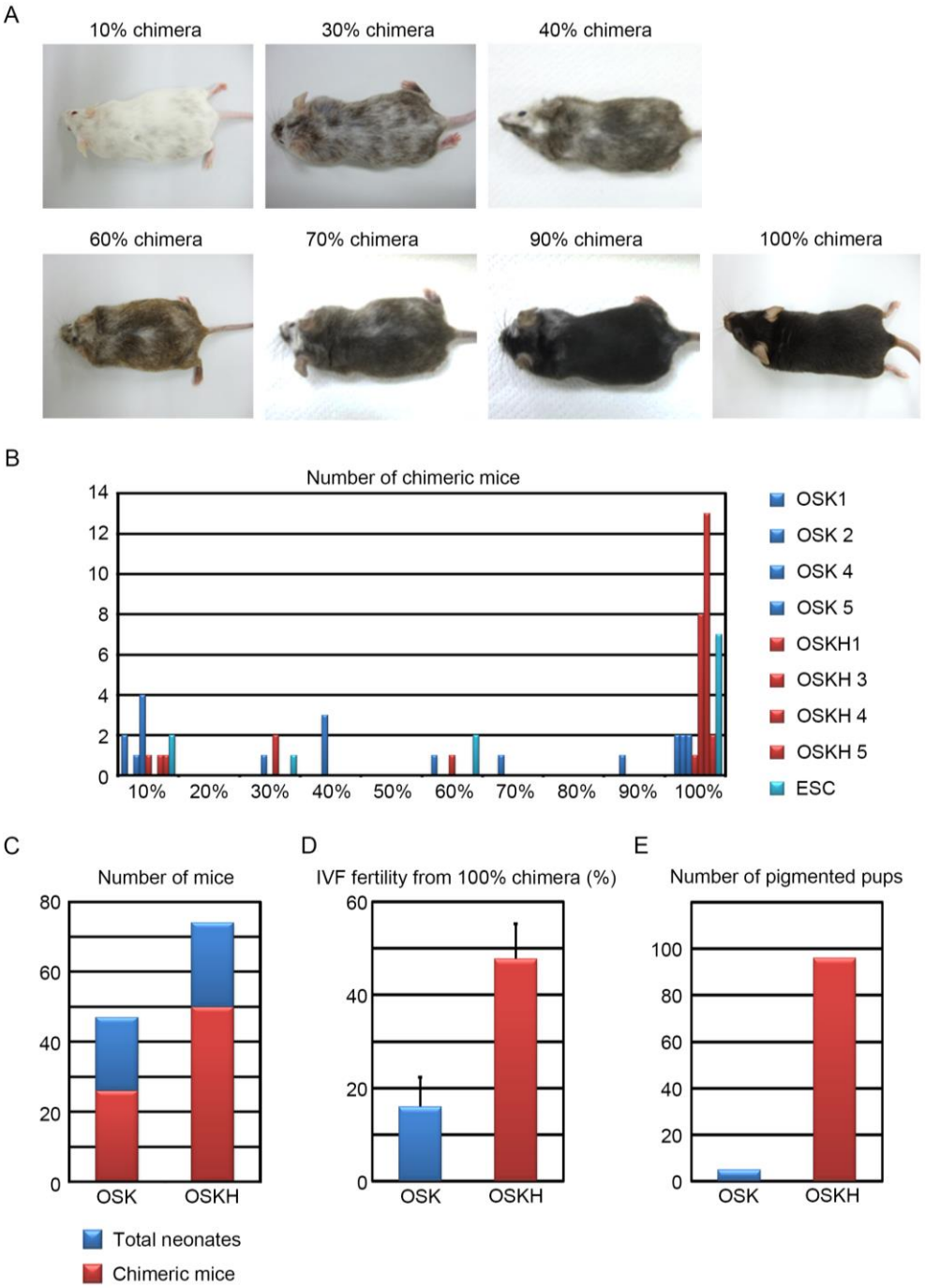

(A) Images of representative chimeras with agouti coat color indicating iPSC origin. (B) Number of agouti coat colored chimeric mice derived from each iPSCs and ESCs. (C) Number of total neonates and chimeric mice from each four replicates of iPSCs. (D) IVF fertility from 100% chimeric mice derived from each four replicates of iPSCs. Error bars represent the SEM. (E) Number of pigmented pups of each coat color from 100% chimeric mice derived from each four replicates of iPSCs.

Table S1.

Primers for qRT-PCR

	Forward	Reverse
Nanog	AGGGTCTGCTACTGAGATGCT	CAACACCTGGTTTTTCTGCCACCG
Oct4 (Endogenous)	TCTTTCCACCAGGCCCCCGGCTC	TGCGGGCGGACATGGGGAGATCC
Sox2 (Endogenous)	TAGAGATAGACTCCGGGCGATGA	TTGCCTTAAACAAGACCACGAAA
Oct4 (Transgene)	CCCCAGGGCCCCATTTTGGTACC	CCCTTTTTCTGGAGACTAATAAA
Sox2 (Transgene)	GGCACCCCTGGCATGGCTCTTGGCTC	TTATCGTCGACCACTGTGCTGCTG
Rex1	ACGAGTGGCAGTTTCTTCTTGGGA	TATGACTCACTTCCAGGGGGCACT
Sall4	CCCTGGGAACTGCGATGAAG	TCAGAGAGACTAAAGAACTCGGC
H1foo	GGCACAGGCTTTCTTTGTCT	TCCAACACAAGTACCCGACA
Foxa2	AGCACCATTACGCCTTCAAC	CCTTGAGGTCCATTTTGTGG
Cxcr4	CGGGATGAAAACGTCCATTT	ATGACCAGGATCACCAATCCA
Col6a2	CCACCACTGAAAGGAACAACAA	TCCAACACGAAATACACGTTGAC
T	TGTCCTCCCTTGTTGCCTTA	ATGTTCCAAGGGCAGAACAG
β3-Tubulin	CCCAGCGGCAACTATGTAGG	CCAGACCGAACACTGTCCA
Otx2	CCAAATCTACCCACCAAGGA	AGAGCTTCCAGAACGTCGAG
Ki67	TCTGATGTTAGGTGTTTGAG	CACTTTTCTGGTAACTTCTTG
PCNA	TAAAGAAGAGGAGGCGGTAA	TAAGTGTCCCATGTCAGCAA
GAPDH	TTCAACGGCACAGTCAAGG	CATGGACTGTGGTCATGAG
Lgals3bp	GCTGGAACTATGGCTTCTCG	GAGCCTTCAAAGCTGGTGAC
FST	GCAGCCGGAACTAGAAGTACA	ACACAGTAGGCATTATTGGTCTG
Dap	TTACCAGGCTGTGTCGCTA	TTATGGCTTTAAGGTCCCTTCCTA
Lnx1	ATGAAGGCGCTGCTGCTTCTGG	CGCTCTCA AGATGGCTGTCCTG
Grik3	TGGAACCCTACCGCTACTCG	TGCGACGCTCGCTGGTAGCA
Aoc1	GCGTGTTGCCTATGAGGTCAG	AAAGCATCCAGGAAAGTAGCG
Crygc	TGCTGCCTCATCCCCCAACA	TCGCCTAAAGAGCCAACTT
1500009C09Rik	TCATTACTTGACTTTGCACAC	GCAAAGGTGGCCATAGAACC
Nr0b1	ACCGTGCTCTTTAACCCAGA	CCGGATGTGCTCAGTAAGG
SSEA1	AGCTTTGCAGTGCACATCAC	AACCAGTCTGCCAAGTTGTG
EpCAM	AGGGGCGATCCAGAACAACG	ATGGTCGTAGGGGCTTTCT
Col1a1	GACGCCATCAAGGTCTACTG	ACGGGAATCCATCGGTCA
Vcam1	TGCCGAGCTAAATTACACATTG	CCTTGTGGAGGGATGTACAGA

Primers for bisulfite sequence

Oct4-DMR	GGTTTTTTAGAGGATGGTTGAGTG	TCCAACCCTACTAACCCATCACC
Nanog-DMR	GATTTTGTAGGTGGGATTAATTGTGAATTT	ACCAAAAAAACCCACACTCATATCAATATA

Primers for pyrosequence

IG-DMR	GTGGTTTGTTATGGGTAAGTTT	CCCTTCCCTCACTCCAAAAATTAA
Gtl2-DMR	AGTTATTTTTTGTTTGAAAGGATGTGTA	CTAACTTTAAAAAAAAATCCCCAACACT

Supplemental Experimental Procedures

Generation of mouse iPSCs and cell culture

The generation of mouse iPSCs was based on a published protocol (Takahashi et al., 2007). We generated iPSCs from tale tip fibroblasts of C57BL/6J mouse using a pMXs retroviral vector with *Oct4*, *Sox2*, *Klf4*, and *H1foo* or *DsRed* as a control. The mouse ES cells (B6J-23^{UTR}) (Tanimoto et al., 2008) were obtained from the Laboratory Animal Resource Center at the University of Tsukuba and were used in accordance with the Guidelines for Derivation and Utilization of Human Embryonic Stem Cells of the Ministry of Education, Culture, Sports, Science, and Technology, Japan. These cell lines were cultured in mouse iPSC medium consisting of DMEM (Sigma-Aldrich, MO, USA) supplemented with 20% KnockOut Serum Replacement (Gibco, CA, USA), 1 mM GlutaMAX (Gibco), 1 mM Non-Essential Amino Acids (Sigma-Aldrich), 0.1 mM 2-mercaptoethanol, 50 U penicillin, 50 mg/ml streptomycin (Gibco), and mouse leukemia inhibitory factor. The iPSC and ESCs were maintained on irradiated mouse embryonic fibroblast (iMEF) feeder cells from wild-type ICR mice in mouse iPSC medium, which was changed every 2-3 days, and the cells were passaged using 0.5 mM trypsin-EDTA (Gibco) every 2-3 days.

Nanog-GFP mouse

We generated iPSC from tale tip fibroblasts of *Nanog*-GFP-IRES-puro transgenic mice (Okita et al., 2007) using the same protocol as described above. The iPSCs generated with the *Nanog*-GFP transgene were positive for GFP, and we counted GFP positive ES-like colonies on day 21 after retroviral infection. Animal care was in accordance with the guidelines of Keio University for animal and recombinant DNA experiments.

Plasmid construction

H1foo cDNA (Teranishi et al., 2004) was inserted into the BamH1 and Sal1 sites of the pMXs plasmid. *H1a* cDNA (Lin et al., 2013) and *H1c* cDNA (Teranishi et al., 2004) was inserted into the EcoR1 and Sal1 sites of the pMXs plasmid. The plasmids were confirmed by DNA sequencing.

Embryoid body formation

The iPSCs and ESCs were harvested with 1 mg/ml collagenase IV, and we transferred 5×10^4 cells into 100 mm low attachment plates (AGC, Tokyo, JAPAN) containing differentiation medium. The differentiation medium consisted of Minimum Essential Medium Alpha Medium (Gibco) supplemented with 20% fetal bovine serum (Gibco), 2 mM GlutaMAX (Gibco), 0.1 mM Non-Essential Amino Acids (Sigma-Aldrich), 0.1 mM 2-mercaptoethanol, 50 U/ml penicillin and 50 mg/ml streptomycin (Gibco). The medium was replaced every 2-3 days. The time window of differentiation for analyzing the size and number of embryoid bodies was 5 days from the beginning of the differentiating conditions.

Teratoma formation

The iPSCs were injected into the testis of SCID mice (CLEA, Tokyo, JAPAN). Prior to injection, mice were anesthetized using a mixture of ketamine (50 mg/kg), xylazine (10 mg/kg), and chlorpromazine (1.25 mg/kg). Adequate anesthesia was maintained by monitoring the heart rate, muscle relaxation, and loss of sensory reflex response (i.e., no response to tail pinching) in mice. At approximately 8 weeks after injection, mice were sacrificed by cervical dislocation, and the teratomas were dissected, fixed in 10% paraformaldehyde (PFA) overnight, and embedded in paraffin. The sections were stained with hematoxylin and eosin. ~~All experiments were performed in accordance with the Keio University Animal Care Guidelines and were approved by the Ethics Committee of Keio University (20-041-4), which conforms to the Guide for the Care and Use of Laboratory Animals published by the US National Institutes of Health.~~

Coculture aggregation of ESCs and iPSCs

Two-cell embryos were collected from ICR (CD-1®) female mice that had been superovulated and mated naturally and were then cultured to the blastocyst stage. ESCs and iPSCs were dissociated with 0.25% trypsin just before coculture aggregation, and 15 to 20 cells were aggregated with 8-cell blastomeres from which the zonae pellucidae had been removed. Manipulated chimeric embryos were transferred at the blastocyst stage into the uterine horns of ICR pseudopregnant mice at 2.5 d postcoitus.

Immunohistochemistry

The iPSCs and fibroblasts plated on glass bottomed dishes (AGC) were washed once with PBS and fixed with 4% paraformaldehyde (MUTO Pure Chemicals, Tokyo, JAPAN) at 4°C for 15 min. After fixation, the cells were permeabilized with 0.5% Triton X-100 in PBS for 10 min at room temperature. After blocking with ImmunoBlock (DS Pharma Biomedical, Osaka, JAPAN) for 20 min, the cells were incubated at room temperature for 60 min with the primary antibodies, followed by washing with the blocking medium and incubation at room temperature for 60 min with the corresponding secondary antibodies. Immunostaining was performed with the following primary antibodies and reagents: Nanog (RCAB0001P, ReproCELL, Kanagawa, JAPAN), SSEA1 (sc-21702, Santa Cruz Biotechnology, CA, USA), H1foo (HPA037992, Sigma-Aldrich), and 6-Diamidino-2-Phenylindole (DAPI, Life Technologies, CA, USA). The secondary antibodies used included anti-rabbit IgG and anti-mouse IgG or IgM conjugated with Alexa Fluor 488 or Alexa Fluor 568 (Life Technologies). The signal was detected using a conventional fluorescence laser microscope equipped with a color charge-coupled device camera (BZ-9000 KEYENCE, Osaka, JAPAN), optical microscope (IX71, Olympus) and laser confocal microscope (LSM 510 META, Carl Zeiss, Jena, Germany).

Electron microscopy

Control and *H1foo* overexpressed fibroblasts were fixed with 2.5% glutaraldehyde in 60 mM HEPES, pH 7.4 for 2 hours at 4°C, and washed three times with 0.2 M Phosphate buffer. Secondary fixation was performed by 1% OsO4 in 60 mM HEPES, pH 7.4 for 120 min. at 4°C. For en bloc stain, 2% uranyl acetate was used for 30 min. at 4°C. Tissues were dehydrated with gradually increasing concentration of ethanol and embedded by plain resin, before sectioning and staining.

Quantitative RT-PCR analysis

Total RNA samples were isolated using the TRIZOL reagent (Life Technologies) according to the manufacturer's instructions. The concentration and purity of the RNA samples were determined with an ND-1000 spectrophotometer (Thermo Fisher Scientific, MA, USA), and cDNA was synthesized with ReverTra Ace qPCR RT Master Mix (TOYOBO, Osaka, JAPAN). Quantitative PCR (QT-PCR) was performed with a 7500 real-time PCR system (Life Technologies) with SYBR Premix ExTaq (TaKaRa, Shiga, JAPAN). The amount of mRNA was normalized to the amount of GAPDH mRNA. The primer sequences are listed in Table S1.

Apoptosis assay

On day 1 after initiating the differentiating conditions, embryoid bodies from iPSCs were trypsinized and suspended in annexin A5 binding buffer. Single cells were stained with annexin-A5-FITC and propidium iodide (BD, CA, USA) according to the manufacturer's protocol. Cells were filtered through 70 mm pore nylon membranes and analyzed by FACS Aria3 (BD) flow cytometry using CellQuest software (BD). Finally, the data obtained were analyzed with FlowJo software (Tree Star, CA, USA).

DNA methylation analysis

For the bisulfite sequence, genomic DNA was extracted from bulk cell culture samples by a SV Genomic DNA purification kit (Promega, Madison, WI, USA). Purified genomic DNA was used as the input for bisulfite conversion with an EZ DNA Methylation-Gold Kit (ZYMO RESEARCH, CA, USA) according to the manufacturer's protocol. For each bisulfite PCR, TaKaRa EpiTaq HS (TaKaRa) was used to catalyze amplification. PCR was performed with the following thermal cycling conditions: denaturation at 98°C for 10 min and 40 cycles, each cycle comprising incubation at 95°C for 20 sec, 55°C for 30 sec, and 72°C for 60 sec, followed by a final extension for 5 min at 72°C. The primers used for bisulfite PCR are listed in Table S1. For sequencing, the purified PCR products were TA-cloned into the pGEM-T vector (Promega). For pyrosequencing, genomic DNA was extracted and bisulfite converted as described above. PCR products were sequenced, and the methylation status of each locus was analyzed using PyroMark Q24 (QIAGEN, Venlo, Netherlands) following the manufacturer's instructions.

Global gene expression analysis

Total RNA was isolated from iPSCs and ESCs. Cyanine-labeled antisense RNA was amplified using the Quick Amp Labeling Kit (Agilent Technologies, CA, USA), hybridized with the Gene Expression Hybridization Kit onto a Whole Mouse Genome Oligo Microarray (Agilent Technologies), and analyzed using the Agilent Microarray Scanner. The data were analyzed with GeneSpring GX12.0 software (Agilent Technologies). ~~Microarray data are available through GEO accession number GSE79515.~~

Accession number

The accession number for the microarray data reported in this paper is GSE79515.

Statistical analysis

Values are reported as the means ± SEM. The data were analyzed using StatView J-4.5 software. Comparisons between two groups were performed with Student's *t*-test or Mann-Whitney test. Comparisons among groups were performed by one-way ANOVA with Bonferroni's *post hoc* test or Benjamini-Hochberg method. The probability level accepted for significance was * $P<0.05$, ** $P<0.01$.

Supplemental References

Lin, C.J., Conti, M., and Ramalho-Santos, M. (2013). Histone variant H3.3 maintains a decondensed chromatin state essential for mouse preimplantation development. Development *140*, 3624-3634.

Okita, K., Ichisaka, T., and Yamanaka, S. (2007). Generation of germline-competent induced pluripotent stem cells. Nature *448*, 313-317.

Takahashi, K., Okita, K., Nakagawa, M., and Yamanaka, S. (2007). Induction of pluripotent stem cells from fibroblast cultures. Nature protocols *2*, 3081-3089.

Tanimoto, Y., Iijima, S., Hasegawa, Y., Suzuki, Y., Daitoku, Y., Mizuno, S., Ishige, T., Kudo, T., Takahashi, S., Kunita, S.*, et al.* (2008). Embryonic stem cells derived from C57BL/6J and C57BL/6N mice. Comparative medicine *58*, 347-352.

Teranishi, T., Tanaka, M., Kimoto, S., Ono, Y., Miyakoshi, K., Kono, T., and Yoshimura, Y. (2004). Rapid replacement of somatic linker histones with the oocyte-specific linker histone H1foo in nuclear transfer. Developmental Biology *266*, 76-86.